Molecular Crystals and Liquid Crystals
Publication details, including instructions for authors and subscription information:
http://www.tandfonline.com/loi/gmcl20

Thin Nematic Films: Laboratory of Physics for Topological Defects

Dalija Jesenek [a], Ivan Gerlic [b], Anja Visnikar [b], Robert Repnik [b] & Samo Kralj [a b]

[a] Jožef Stefan Institute, Jamova 39, SI-1000, Ljubljana, Slovenia

[b] Faculty of Natural Sciences and Mathematics, University of Maribor, Koroška cesta 160, SI-2000, Maribor, Slovenia

Available online: 11 Jan 2012

To cite this article: Dalija Jesenek, Ivan Gerlic, Anja Visnikar, Robert Repnik & Samo Kralj (2012): Thin Nematic Films: Laboratory of Physics for Topological Defects, Molecular Crystals and Liquid Crystals, 553:1, 153-160

To link to this article: http://dx.doi.org/10.1080/15421406.2011.609461

Mol. Cryst. Liq. Cryst., Vol. 553: pp. 153–160, 2012

ISSN: 1542-1406 print/1563-5287 online
DOI: 10.1080/15421406.2011.609461

Taylor & Francis
Taylor & Francis Group

Thin Nematic Films: Laboratory of Physics for Topological Defects

DALIJA JESENEK,[1] IVAN GERLIC,[2,*] ANJA VISNIKAR,[2] ROBERT REPNIK,[2] AND SAMO KRALJ[1,2]

[1]Jožef Stefan Institute, Jamova 39, SI-1000 Ljubljana, Slovenia
[2]Faculty of Natural Sciences and Mathematics, University of Maribor, Koroška cesta 160, SI-2000 Maribor, Slovenia

In this pedagogical presentation we demonstrate basic physics of topological defects in orientational ordering. We limit to two dimensional (2D) films. Different defect structures and pairs defect-antidefect are visualized in the applet presentation, which shows also the corresponding interference textures simulating typical polarizing microscopy experiment. The conservation of topological defect is shown on the case of 2D films on curved surfaces. In different geometrical shapes with the same Euler characteristics we demonstrate equilibrium (or at least relatively stable) nematic structures possessing 2 to 8 defects pairs with the winding number $|\mathrm{M}| = 1/2$*, where the sum of all defects corresponds to* $\mathrm{M}_{\mathrm{tot}} = 2$*.*

Keywords Didactics of physics; topological defects; nematic liquid crystals; nematic shells

1. Introduction

Topological defects have attracted scientists' interest for years. They are ubiquitous, being retraced in different branches of physics, such as condensed matter physics, particle physics and cosmology. The first theory of topological defects was indeed proposed by cosmologists [1] to explain the coarsening dynamics of the defect tangle in the early universe. Now, it is also believed that they significantly influence the structure of universe. For example, they might be good candidates to unveil the mystery of dark matter [2]. On the other hand, they play an important, documented role in several applications, among which some are in nano-based technology [3].

Defects are classified into different classes according to their topological charge by the homotopy group theory [4]. This charge is a conserved quantity and controls the transformations of defects (merging, annihilation, decaying). Therefore, an isolated defect with a finite topological charge is topologically stable and cannot by itself be continuously unwound, leaving no trace behind.

Due to their softness, liquid character and anisotropic optical properties liquid crystal (LC) phases and structure are particularly appropriate media to study many classes of defects [5]. In this contribution we present essential properties of defects in the nematic LC

*Address correspondence to Ivan Gerlic, Faculty of Natural Sciences and Mathematics, University of Maribor, Koroška cesta 160, SI-2000 Maribor, Slovenia. E-mail: ivan.gerlic@uni-mb.si

phase. The main purpose of our educational presentation is to present different defects and their stability. The presentation content is focused on undergraduate students of physics-educational branch.

The content of the paper is as follows. In Sec. 2 we present nematic defects is thin LC films. We first consider different structures of defects in a flat film. Then we show some examples on curved surface where different number of defects could be stabilized. In the last section we summarize the content of the presentation.

2. Main Characteristics and Stability of Defects

2.1 Topological Characteristics

We first illustrate different possible defect structures in orientational ordering and their main topological characteristics. For illustration purposes we use the simplest possible presentation and consider rod-like LC molecules. The nematic orientational ordering is described in terms of the nematic director field $\vec{n}$ pointing along a local average orientation. The two dimensional (2D) model is considered where the nematic LC phase is confined within a thin plan-parallel cell lying in the (x,y) plane of the Cartezian coordinate system. In 2D main topological properties are described by the winding number M (also called the Frank index) [6], which in this specific case is equivalent to the topological charge. It is defined in terms of $\vec{n}$ surrounding the defect: $M = \phi_{eff}/(2\pi)$. Here ϕ_{eff} describes the effective rotation of $\vec{n}$ on encircling the defect origin in the clock-wise direction. Because of symmetry reasons the winding number can have only half integer or integer values [6]. Therefore $M = \pm$ 1/2, $\pm$ 1, $\pm$ 3/2, $\pm$ 2.... The total winding number of a system is a conserved quantity. A pair of defects of opposite winding numbers $\pm M$ is commonly referred to as a "defect" ($M > 0$) and "antidefect" ($M < 0$). Such defect-pairs can potentially annihilate each other into a defectless state.

In the (x,y) plane one commonly parametrizes the director field as $\vec{n} = (\sin\theta, \cos\theta)$. The elastic free energy density f_e is in the simplest case (the so called approximation of equal nematic elastic constants) expressed as [6]

$$f_e = \frac{K}{2}\left(\left(\frac{\partial\theta}{\partial x}\right)^2 + \left(\frac{\partial\theta}{\partial y}\right)^2\right). \tag{1}$$

where K is the representative nematic elastic constant. The corresponding Euler-Lagrange equation reads $\frac{\partial^2\theta}{\partial x^2} + \frac{\partial^2\theta}{\partial y^2} = 0$. The solution describing a family of defect structures is given by

$$\theta(x, y) = MArcTan\left(\frac{x - x_i}{y - y_i}\right) + C. \tag{2}$$

The origin of a defect is determined by (x_i,y_i), M is the winding number and C is a constant. The corresponding free energy density reads

$$f_e = KM^2/(2\rho^2), \tag{3}$$

where $\rho = \sqrt{(x - x_i)^2 + (y - y_i)^2}$. Note that LC avoids the singularity at the defect's origin ($\rho = 0$) by melting, which consequently yields $K = 0$. In order to describe the defect core configuration description of LC order in terms of the tensor order parameter is required [6].

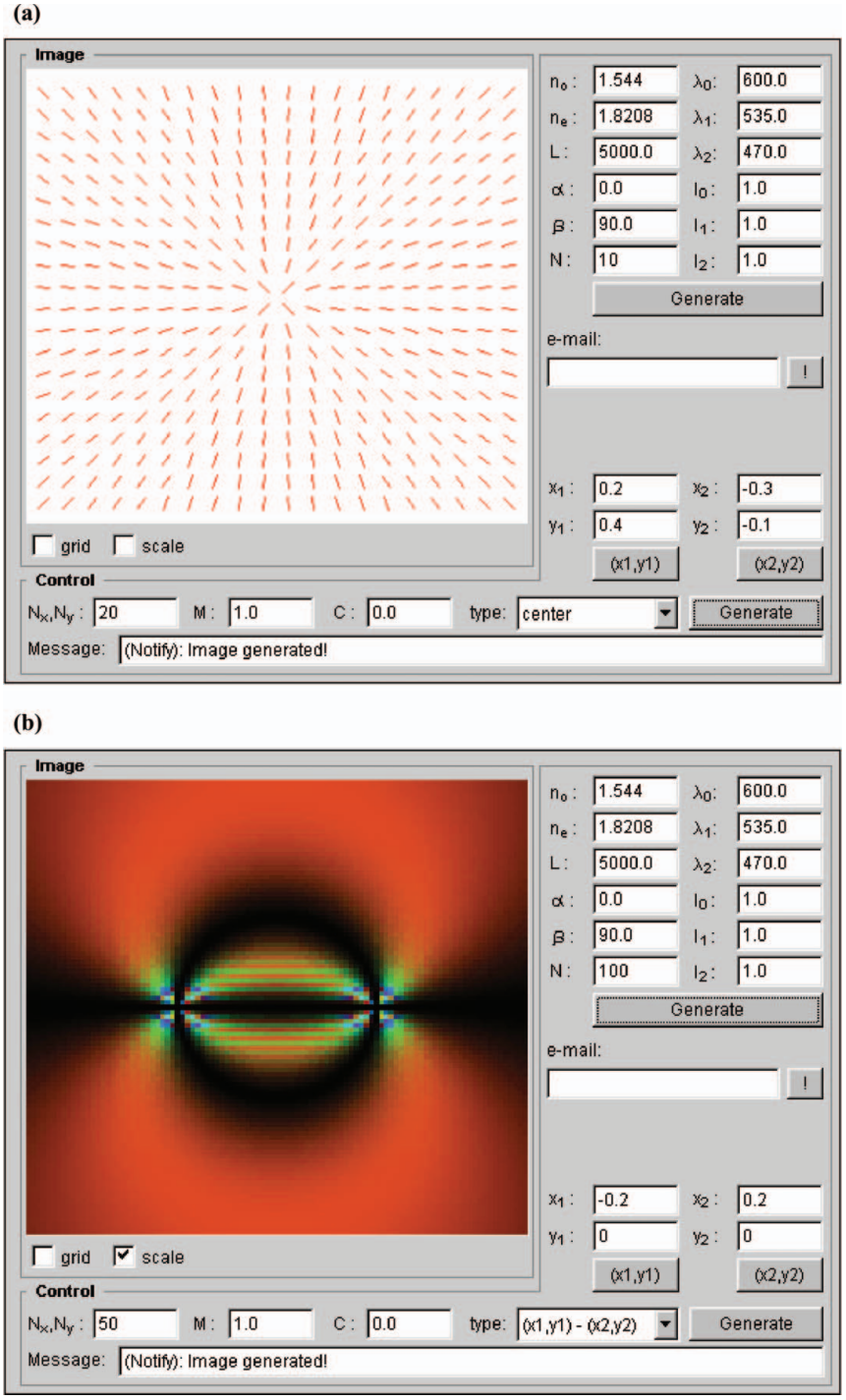

Figure 1. The applet presentation of different defect structures in 2D flat film (see [7]). (a) The director field distribution of the defect with $M = 1$. (b) Calculated typical interference pattern of a pair of defects $M = 1$ and $M = -1$, which simulates polarizing microscopy experiment.

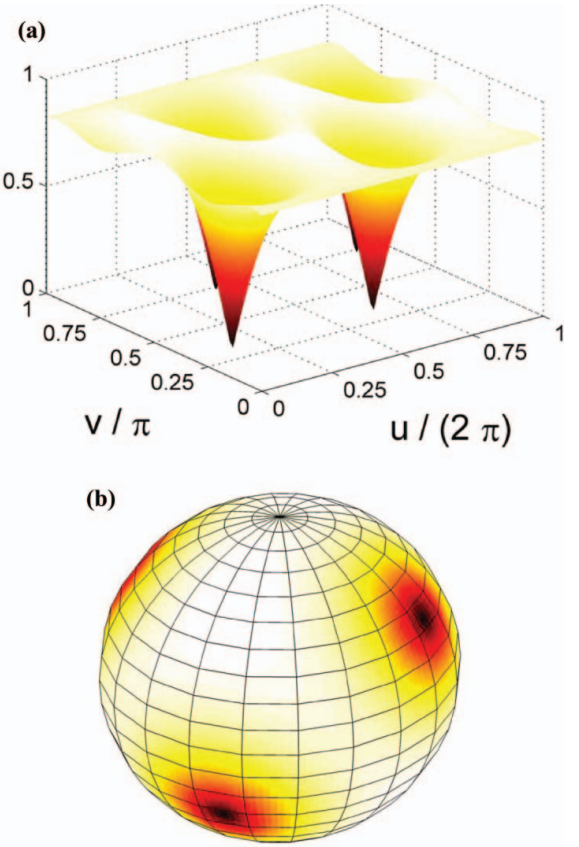

Figure 2. Graph showing variation of λ on a nematic film covering a sphere. (a) The two dimensional $\lambda = \lambda(u, v)$ dependence. We show the example where the radius of the sphere is about order of magnitude larger with respect to the nematic order parameter correlation length. The defect sites are signaled by $\lambda = 0$ and λ_c determines value of in an undistorted LC film. (b) The corresponding λ spatial variation in 3D Cartezian coordinate system.

We further emphasize that $f_e \propto M^2$. Therefore from energy point defects possessing low values of M are favored.

Different defects structures (single defects and pairs defect-antidefect) in 2D on varying M and C and corresponding typical interference patterns obtained in a polarization microscopy experiment are presented in our applet [7]. Its content is described in detail in [8]. In Fig. 1 we show some illustrative examples. In Fig. 1a is depicted a defect characterized by $M = 1$. In Fig. 1b we show interference texture of a pair $M = 1$ and $M = -1$.

2.2 Stability of defect structures

The total topological charge, i.e., the total winding number M_{tot} in 2D, is determined by the Euler characteristics $s\chi$ of the surface. For the closed surface it can be expressed as [9]

$$\chi = V - E + F = \oiint K_g d\vec{r}^2, \tag{4}$$

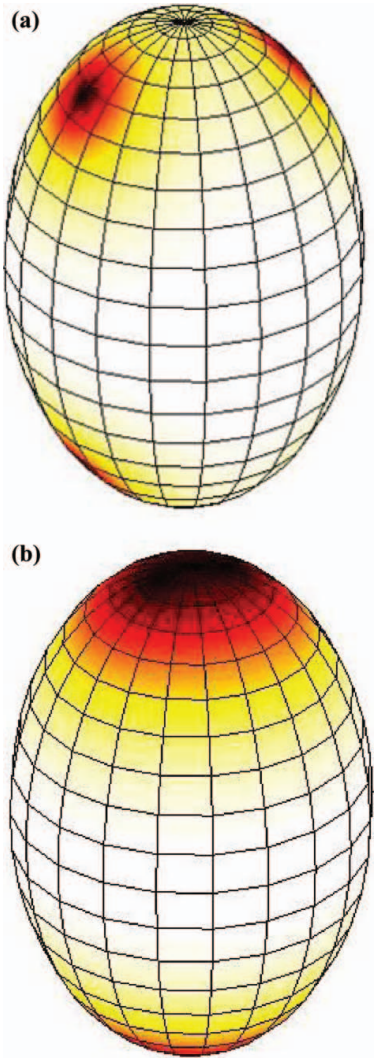

Figure 3. Defects residing on elliptical surface. Depending on the ration a/b there could be either 2 or 4 defects. (a) 4 defects with $M = 1/2$, a/b = 1.5. (b) 2 defects with $M = 1$, a/b = 3.

where V, E, and F stand for the numbers of vertices (corners), edges and faces of polyhedrons for a given polygonization of the surface, and K_g stands for the Gauss curvature of the surface, respectively. In 2D it further holds $\chi = M_{tot}$. For example, for surfaces isomorphic to a sphere or to a torus, it holds $\chi = 2$ and $\chi = 0$, respectively.
In order to study defect configurations and their defect structures in thin films it is convenient to use the parametrization [10]

$$Q = \lambda(\vec{n} \otimes \vec{n} - \vec{n}_\perp \otimes \vec{n}_\perp). \tag{5}$$

The order parameter Q is expressed in the diagonal form, where the orthogonal unit vectors $\vec{n}$ and $\vec{n}_\perp$ lie within a film. The quantity λ measures the degree of nematic ordering on the surface described by the coordinates (u,v). More details about Q and the corresponding

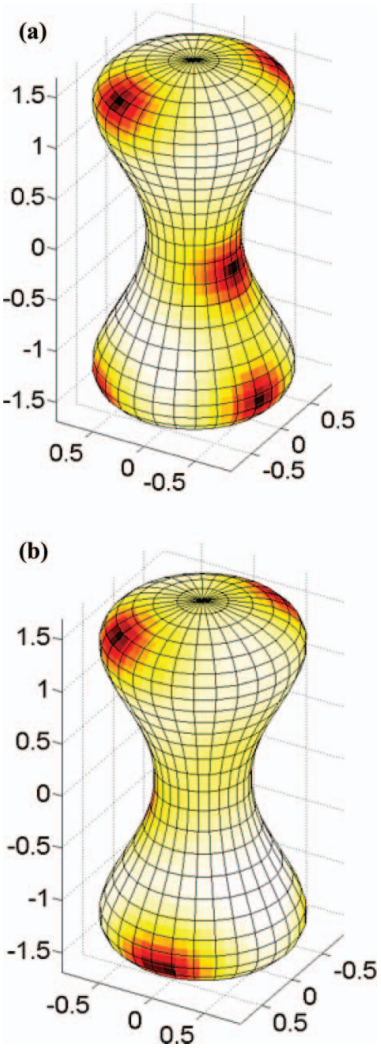

Figure 4. Defects residing on curved surface. In the case shown 6 defects are stable. The total sum of winding numbers equal $M_{\text{tot}} = 2$. In (a) and (b) we show the configurations from different perspectives. a = 1.69, b = 0.8, $\Delta b = 0.4$.

theory, which has been developed by E.G. Virga and R. Rosso, is given in [10]. Below we present some structures that are calculated using this approach. The $\lambda\,(u, v)$ surface plots well reveal topological defects and their core structure. Namely, at defect origins it holds $\lambda = 0$. Below we present some spatial variations of λ on surfaces of revolution described by

$$\vec{r} = \rho(v)\cos(u)\,\vec{e}_x + \rho(v)\sin(u)\,\vec{e}_y + z(v)\,\vec{e}_z, \tag{6}$$

where the unit vectors $\vec{e}_x, \vec{e}_y, \vec{e}_z$ define directions of the Cartezian coordinate system (x,y,z), and $u \in [0, 2\pi]$. In Fig. 2 we show a two-dimensional plot of λ on an ellipsoid, which is

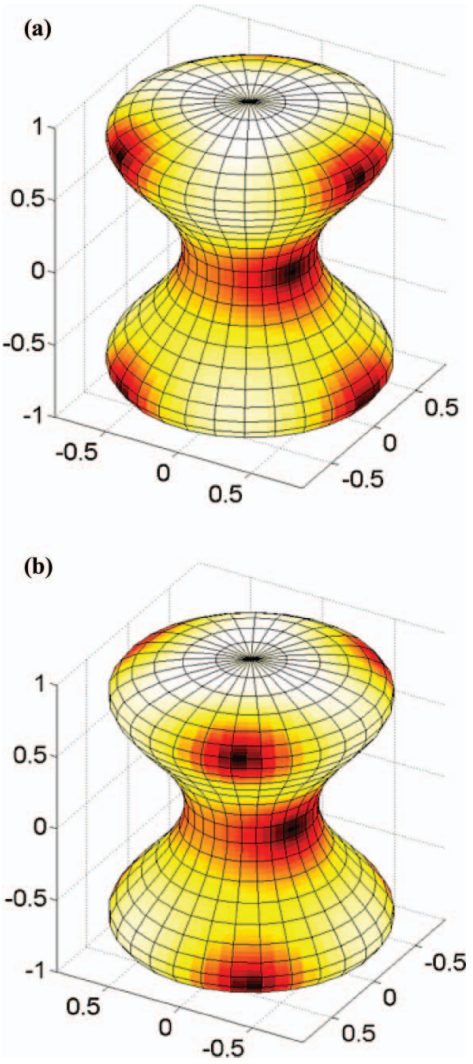

Figure 5. Defects residing on curved surface. The case with 8 defects is shown. The total sum of winding numbers equals $M_{\text{tot}} = 2$. In (a) and (b) we show the configurations from different perspectives. a = 1.0, b = 0.8, $\Delta b = 0.4$.

parametrized as

$$\rho(v) = b\sin(v),\ \ z(v) = a\cos(v), \tag{7}$$

$v \in [0, \pi]$. In Fig. 2a we show $\lambda(u, v)$ variation, which clearly reveals four defects. They are all characterized by $M = 1/2$, thus $M_{tot} = 2$. In Fig. 2b we plot the corresponding λ variation in the Cartezian coordinate system. Colored regions reveal the presence of defects.

Rough analysis suggests (see Eq. (3)) that in thin films defects with $|M| = 1/2$ are favored and that there is tendency to minimize number of defects. We next demonstrate that by varying geometrical details and elastic constants different numbers of defects appear in equilibrium configurations. For this purpose we confine our interest to geometries

isomorphic to a sphere, characterized by $M_{tot} = 2$. In Fig. 3b we show the case with two defects bearing M = 1, which is driven geometrically by imposing $a >> b$ (for details see [10]). The configuration of 4 defects is stable only below a critical value of the ratio a/b (see Fig. 3a), which depends also on temperature and LC material properties.

In Figs. 4 and Figs. 5 the cases with 6 and 8 defects are shown, respectively. In these geometries we used the parametrization

$$\rho(v) = b\sin(v) + \Delta b\sin(3v),\ \ z(v) = a\cos(v). \tag{8}$$

The appearance of additional defects was triggered either by changing the geometry or elastic constants. In this respect, an important role is also played by the saddle splay constant k_{24} (for details see [10]). In Fig. 4 the winding numbers of defects are as follows. The two defects at the upper part and the three defects at the bottom region all bear $M = 1/2$. On the contrary the defect in the equatorial region possesses $M = -1/2$. Fig. 5: The three defects at the upper part and the three defects at the bottom region all bear $M = 1/2$. The two defects in the equatorial region posses $M = -1/2$.

3. Summary

In our educational presentation we demonstrate basic characteristics of topological defects in nematic ordering in thin nematic films. In this case the main topological characteristics are played by the winding number M. The total winding number M_{tot} is the conserved quantity and is determined by the Euler characteristics of the surface. Different defect structures are shown in the applet presentation [7] in terms of the nematic director field. The typical corresponding interference textures are also shown, which could be obtained in conventional polarizing microscopy experiment. The defect conservation, merging and splitting are demonstrated on curved surfaces exhibiting cylindrical symmetry. The 2D formalism in terms of tensor order parameter Q was used which has been recently developed by Pavia group [10]. Using it the cores of defects are well visualized. Furthermore, at defect sites the eigenvector λ of Q vanishes. We study different geometries which are isomorphic to a sphere. In this case $M_{\text{tot}} = 2$. We show equilibrium (or quasi equilibrium) cases where total number of defects equals 2, 4, 6 or 8. The defects posses either $M = 1/2$ or $M = -1/2$.

References

[1] Kibble, T. W. B. (1976). *J. Phys. A*, *9*, 1387.
[2] Nukamendi, U., Salgado, M., & Surarsky, D. (2000). *Phys. Rev. Lett.*, *84*, 3037.
[3] Song, W., Kinloch, I. A., & Windle, A. H. (2003). *Science*, *302*, 1363.
[4] Mermin, N. (1979). *Rev. Mod. Phys.*, *51*, 591.
[5] Kurik, M. V., & Lavrentovich, O. D. (1988). *Usp. Fiz. Nauk.*, 154.
[6] De Gennes, P. G., & Prost, J. (1993). The Physics of Liquid Crystals, Oxford: Oxford University Press.
[7] http://samo.kralj.fnm.uni-mb.si/files/applet/start.html
[8] Kaučič, B., Ambrožič, M., & Kralj, S. (2004). *Eur. J. Phys.*, *25*, 515.
[9] Kamien, R. D. (2002). *Rev. Mod. Phys.*, *74*, 953.
[10] Kralj, S., Rosso, R., & Virga, E. G. (2011). *Soft matter*, *7*, 670.